Infrared optical constants of low-temperature H2SO4 solutions representative of stratospheric sulfate aerosols

Robert T. Tisdale, David L. Glandorf, and Margaret A. Tolbert

Department of Chemistry and Biochemistry and Cooperative Institute for Research in Environmental Sciences
University of Colorado, Boulder

Owen B. Toon

Laboratory for Atmospheric and Space Physics and Department of Atmospheric and Oceanic Sciences, University of Colorado, Boulder

Abstract. We have determined the infrared optical constants of sulfuric acid solutions at intervals of approximately 5 wt% between 45 and 80 wt% H_2SO_4 at a temperature near 215 K. The optical constants were determined by first measuring the transmission of infrared light (7000 to 500 cm^{-1}) through sulfuric acid films of varying thickness. An iterative Kramers-Kronig technique was then used to determine the optical constants that yielded the best match between calculated and measured spectra. Finally, a fitting routine was used to create a method for interpolating between the sulfuric acid compositions where optical constants were measured. The optical constants determined here differ considerably from those measured at warmer temperatures using reflection techniques. For some frequencies and compositions, the imaginary refractive index is more than twice as large as was previously measured at 300 K. The change in optical constants has significant implications for retrievals of aerosol mass and composition from satellite measurements.

1. Introduction

Sulfuric acid aerosols (SAA) are present throughout Earth's troposphere and stratosphere. Because sulfuric acid is highly hygroscopic, the composition of these aerosols varies greatly with the local relative humidity. As a result, SAA composition is a strong function of the temperature and water partial pressure, as has been modeled in theoretical studies [*Steele and Hamill*, 1981; *Tabazedeh et al.*, 1997]. Tropospheric SAAs can vary between 10 and 70 wt% H_2SO_4 when they are not partially neutralized with ammonia. Stratospheric SAAs are composed of 40 to 80 wt% H_2SO_4 depending on the local conditions.

Recent laboratory studies have shown that several heterogeneous reactions may occur on and in SAAs. Some of these reactions have exhibited composition-dependent kinetics. For example, $ClONO_2$ hydrolysis on 40 wt% H_2SO_4 occurs at a rate more than 100 times greater than it occurs on 75 wt% H_2SO_4 [*Hanson and Ravishankara*, 1991]. Thus, to correctly model the heterogeneous chemistry, the aerosol composition must be accurately known under a variety of atmospheric conditions. Although the composition of sulfuric acid aerosols has been predicted by thermodynamic models, field and laboratory studies of SAAs are needed to verify the accuracy of these models.

In addition to varying with particle composition, chemical reaction rates will increase with particle surface area or particle volume. Satellite measurements of infrared extinction from particles are often used to retrieve these parameters by measuring the size and mass loading of the particles. For example, recent measurements of solar occultation spectra have been made with the atmospheric trace molecule spectroscopy (ATMOS) Fourier transform infrared (FTIR) spectrometer aboard the space shuttle. Attempts to fit these spectra with room temperature optical constants corrected to stratospheric temperatures with the Lorentz-Lorenz relationship led the authors to conclude that the most significant discrepancy between the calculated and measured spectra was caused by errors in the low temperature optical constants of sulfuric acid solutions [*Rinsland et al.*, 1994]. Another study estimated the effective radius, surface density, and volume density of stratospheric aerosols using the emission at 12.1 μm (821 cm^{-1}) measured by the improved stratospheric and mesospheric sounder (ISAMS) instrument. The authors noted that the use of room temperature optical constants limited their certainty in determining the volume, surface area, and effective radius of aerosol particles [*Grainger et al.*, 1995].

Satellite measurements are also used to determine the radiative effect of aerosols. For example, sulfuric acid aerosols are greatly enhanced after volcanic eruptions. In this case, radiative heating of the particles, mainly at infrared wavelengths, has been found to heat the tropical stratosphere and alter stratospheric dynamics significantly [*Kinne et al.*, 1992; *Young et al.*, 1994]. In addition, the aerosols alter the Earth's radiative budget, cooling the surface-atmospheric system [*Minnis et al.*, 1993]. These radiative effects depend upon aerosol mass and surface area.

The optical constants of a material are often referred to as the real and imaginary refractive indices, which can be combined into the complex refractive index, $\hat{n} = n - ik$. Optical constants for sulfuric acid solutions in the atmospheric range of composition have been measured previously under somewhat limited conditions. *Remsberg et al.* [1974] used attenuated total reflection (ATR) infrared spectroscopy to measure

the optical constants at room temperature between 1600 and 750 cm⁻¹ for 75 and 90 wt% H_2SO_4 compositions. *Palmer and Williams* [1975] used a direct reflection technique to measure the optical constants between 27,800 and 400 cm⁻¹ at room temperature for six compositions between 25 and 95.6 wt% H_2SO_4. Finally, *Pinkley and Williams* [1976] measured the optical constants between 6000 and 400 cm⁻¹ at 250 K for 75 and 95.6 wt% H_2SO_4 compositions, again using direct reflection.

Although these studies agree qualitatively with each other, there are some significant differences for 75 wt% H_2SO_4, the one composition at which all three studies made measurements. This is especially true between 750-1000 cm⁻¹, where the imaginary indices of *Remsberg et al.* [1974] for 75 wt% H_2SO_4 are nearly a factor of 2 larger than those of *Palmer and Williams* [1975] and *Pinkley and Williams* [1976] at some frequencies, and between 400-600 cm⁻¹, where the Palmer and Williams imaginary indices are in some cases more than a factor of 2 larger than those measured by Pinkley and Williams. Also, no study has yet determined the optical constants of H_2SO_4 solutions at temperatures below 250 K, although recent studies have shown that the infrared spectra of these solutions change significantly at lower temperatures [*Middlebrook et al.*, 1993; *Anthony et al.*, 1995; *Clapp et al.*, 1997].

We have used transmission FTIR spectra to determine the optical constants of thin films of H_2SO_4, a technique described by *Kozima et al.* [1966]. Several previous measurements of optical constants have been made using this technique [*Verleur*, 1968; *Nilsson*, 1968; *Masterson and Khanna*, 1990; *Pearl et al.*, 1991; *Toon et al.*, 1994]. We have measured the infrared optical constants of H_2SO_4 solutions at approximately 215 K at 5 wt% intervals between 45 and 80 wt% H_2SO_4. For the imaginary refractive index, we report values from 3650 to 500 cm⁻¹, while we report values of the real refractive index from 7000 to 500 cm⁻¹. Finally, we present a scheme for fitting the measured optical constants to allow calculation of optical constants at any composition between 45 and 80 wt% H_2SO_4.

2. Measurements of the Infrared Spectra

The apparatus used to measure the infrared spectra of sulfuric acid solutions has been fully described previously and is depicted in Figure 1 [*Tisdale et al.*, 1997]. Briefly, the infrared spectra were obtained from thin films of H_2SO_4/H_2O condensed onto a cold 50-mm diameter silicon wafer mounted in a vacuum chamber. The films were made by dosing layers of SO_3 and water through leak valves and onto the silicon at low temperature, followed by annealing to form H_2SO_4 [*Middlebrook et al.*, 1993]. Water was admitted to the chamber through a nondirect dosing port, while SO_3 was directly dosed onto the surface to form one-sided films. To form a film, a layer of water approximately 0.07-0.2 μm thick was first dosed onto the silicon at 150 K. Next, a layer of SO_3, followed by another layer of water, was dosed on top of the thin water layer at 150 K. To prevent desorption of the SO_3, the ratio of the thickness of the water film to that of the underlying SO_3 film was approximately 7:1. The thickness of the top two layers was varied in different experiments to obtain different H_2SO_4 film thicknesses. The H_2O-SO_3-H_2O dosing sequence was used to avoid the formation of SO_3 dimers in the film [*Guldan et al.*, 1995]. Finally, the film was warmed in steps to 180 K, then to 210 K to promote reaction to H_2SO_4. Excess H_2O desorbed during the second reaction step, leaving a film of ap-
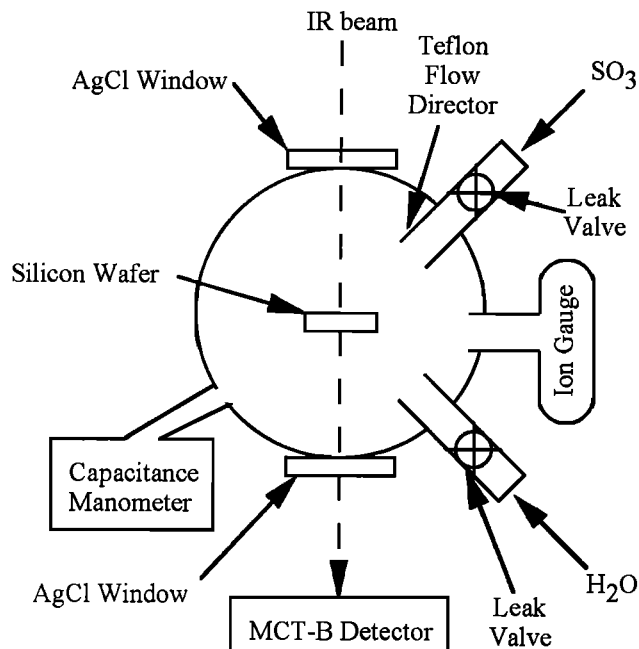
Figure 1. Schematic diagram of the experimental apparatus.

proximately 75-80 wt% H_2SO_4. To obtain more dilute compositions of H_2SO_4, additional water vapor was added to the chamber through a leak valve. The water partial pressure was measured using a capacitance manometer which was zeroed using an ionization gauge.

The temperature of the silicon was measured with type T thermocouple junctions. These thermocouple junctions were attached to a copper heating plate in close thermal contact with the silicon. To correct for any differences in temperature between the silicon and the copper plate, the temperature measurements were calibrated daily using the ice frost point as described by *Iraci et al.* [1995]. The experimentally determined silicon temperatures from the frost points agreed with the thermocouple temperatures to within 6 K. Here we report the thermocouple temperatures of the copper plate corrected to the ice frost point for the silicon.

The infrared absorbances of the films were measured in transmission using collimated light from a Nicolet Magna 550 FTIR spectrometer. The infrared spectra presented here were collected using 4 cm⁻¹ resolution with 16 scans coadded. For the determination of the optical constants, the spectral resolution was reduced to 8 cm⁻¹. An illustration of light passing through the film and substrate is shown in Figure 2. There are an infinite number of reflections at each interface, with some of the light reflected and transmitted each time an interface is encountered. Fortunately, the infinite sum of transmission terms is easily calculated. The optical model used is from *Heavens* [1955] and is fully described by *Toon et al.* [1994]. We have assumed that a slight film exists on the back of the silicon wafer. Because of our direct dosing technique, we expect that very few molecules will stick to the back side of the silicon and that the film will be primarily one-sided. In support of this assumption, double-sided films of nearly equal thickness show optical interference patterns of much higher amplitude than those observed in our experiments. We therefore assume that the thickness on the back side of the silicon is 1% of that on
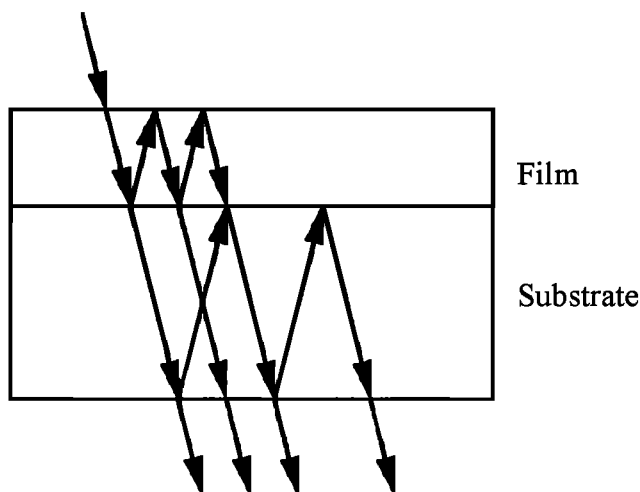
Figure 2. A simplified illustration of the geometry of our experiment. The light strikes the film at normal incidence, but here the light is shown as striking the film at an angle to the normal, so that multiple reflections can be shown. Theoretically, there are an infinite number of reflections at each interface, but only a small number of reflections are shown for clarity.

the front side. This assumption was examined and will be discussed in the section on errors.

The composition of the H₂SO₄ films was varied by changing the water partial pressure in the chamber and in some cases by also changing the temperature of the silicon wafer. In this manner, we were able to obtain film compositions between approximately 45 and 80 wt% H₂SO₄ at temperatures of approximately 215 K. Films of different thicknesses are necessary for the analysis and were obtained in different experiments. Because differences in temperature could not be avoided in different experiments, some films were at slightly different temperatures than others. Table 1 lists the range of film temperatures for each composition.

Because we are unable to determine our film composition directly, the composition of the films was determined using a calibration from infrared spectra of H₂SO₄ films. The model of *Tabazedeh et al.* [1997] was used to calculate the wt% H₂SO₄ from the measured temperature and water partial pressure for a number of data points. The infrared spectral data was then fit to the wt% H₂SO₄ predicted by the model. Only data points where the water pressure and temperature were accurately known were used for the calibration. The composition for all the other data points was then determined using the calibra-
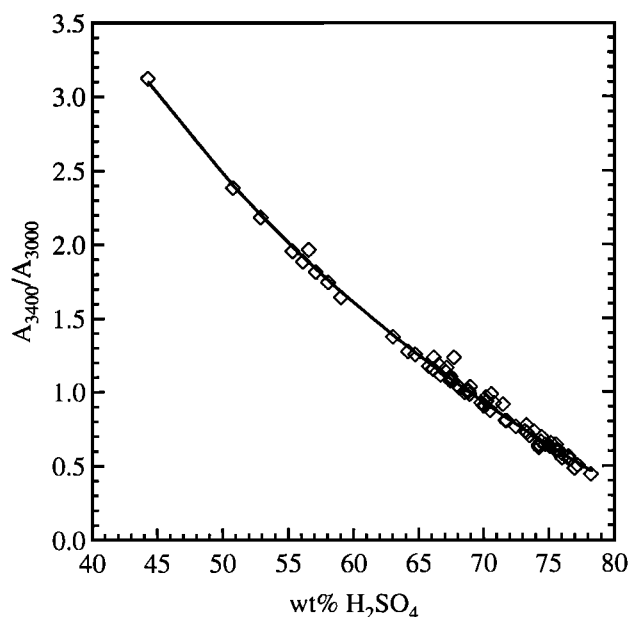
Figure 3. Calibration plot for film composition from thin film spectra. The wt % H₂SO₄ was determined from the model of *Tabazedeh et al.* [1997] using measured temperatures and water partial pressures. Absorbances are from thin film spectra over a range of film thickness. The diamonds are the data, and the solid curve is the fit to the data.

tion. The data used for the calibration were from three separate experiments, each with different film thickness. The film thicknesses ranged from approximately 0.75 to 4.0 μm. The calibration uses two regions of the OH stretching region and a common baseline. Baseline corrected integrated absorbances were calculated for the regions 3450-3350 cm⁻¹ (referred to as A_{3400}) and 3050-2950 cm⁻¹ (referred to as A_{3000}) with a baseline drawn between 3750 and 2400 cm⁻¹. These regions are in the peaks assigned to the O-H stretch for water molecules and for H₂SO₄ molecules, respectively [*Guldan et al.*, 1995]. The ratio of A_{3400} to the A_{3000} was fit as a function of the wt% H₂SO₄ in solution to the following functional form:

$$\frac{A_{3400}}{A_{3000}} = a + \frac{b}{\ln(\text{wt\%}\,H_2SO_4)} \qquad (1)$$

The calibration data used and the fit to the data are shown in Figure 3. The parameters of the fit were a=-17.101 and b=76.592. This calibration was used to calculate the composition of each film from its infrared spectrum and to choose films

Table 1. Characteristics of Films Used in Optical Constant Determinations

Nominal wt%	Number of Films	Film Thickness, μm	Film Coherence	Temperature, K	Composition, wt% H₂SO₄
45.2	3	1.70-4.08	0.31-0.74	203-222	45.2
50.0	3	1 23-2.99	0.58-0.81	209-222	49.9-50.1
55.1	3	1.14-2.57	0 61-0.81	213-222	55.0-55 2
61.6	4	1.04-2.81	0 13-0.82	214-221	61.6-61.7
65.3	5	0.95-2.63	0.31-0.89	214-218	65.2-65.5
70.2	5	0.85-2.36	0.46-0.94	211-218	70.2-70.3
75.0	5	0.76-2.14	0.49-0.96	211-218	75.0
80.0	3	1.07-1.72	0.57-0.73	214-219	79.9-80.0

of similar composition for use in the determination of optical constants.

For each composition studied, the average composition and the range of compositions for the films used in the analysis are listed in Table 1. The 95% confidence limits for this calibration are within 0.3 wt% of the predicted composition.

3. Theory of Optical Constants

The theory used to determine the optical constants has been previously described by *Toon et al.*[1994] and will only be discussed here briefly. We begin our analysis by estimating the thickness and coherence of the films using the optical interference pattern of the spectrum between 3700 and 7000 cm^{-1}. To do this, initial guesses of the optical constants are required. We estimate the real indices by employing a Lorentz-Lorenz temperature correction on the data of *Palmer and Williams* [1975]. This was done using the expression [*Yue and Deepak*, 1981]:

$$n(T) = \sqrt{\frac{2F\rho(T)+1}{1-F\rho(T)}} \qquad (2)$$

where

$$F = \frac{n^2(T_0)-1}{\left[n^2(T_0)+2\right]\rho(T_0)} \qquad (3)$$

and T_0 is a reference temperature at which both n and ρ, the density, are known. The real indices at 300 K from *Palmer and Williams* [1975] were used, and densities were interpolated at 300 K and extrapolated to 215 K using data from *Perry and Green* [1984] from 273-373 K. The Lorentz-Lorenz correction should be a valid approximation as there are no major absorption bands in this spectral region. The imaginary indices of Palmer and Williams were used with linear interpolation between frequencies and compositions. Because the imaginary index is very small in this spectral region, changes due to temperature should have minimal effect on estimation of the film thickness.

The coherence of the film is an approximation used to deal with nonuniformities in film thickness which cause damping of reflected light. This method is discussed more completely in a similar study by *Toon et al.* [1994]. A coherence of 1 indicates that the film is perfectly flat, while a coherence of 0 indicates that the film is uneven enough that no constructive interference is observed. To minimize ripples in the sulfuric acid films, the silicon was mounted horizontally. However, some films were still not perfectly flat. Although the films are supercooled liquid sulfuric acid solutions, the viscosity and surface tension of sulfuric acid solutions at the low temperatures of the film are very high. This can cause slight "beading" of the films which in some cases results in minor loss of coherence of the film. In other cases, it can render the film so incoherent that a calculation of the film thickness is impossible. Therefore incoherent films were not used in our analysis. Visual inspection of the films insured that the films used in the analysis were wetted to the silicon surface, at least on a macroscopic scale. A film which is fairly incoherent (even a coherence of ~0.1) can still show oscillations due to interference. Because the film thickness is determined by the period rather than the amplitude of the oscillation, it is essential that the periods of the oscillations in the measured and calculated spectra are matched. All films used in our analysis showed clear oscillations in the 4000-7000 cm^{-1} region, and the oscillations of the measured and calculated spectra had similar periods. Although coherence may be a frequency dependent parameter, we have assumed that it is independent of the frequency. This may lead to small errors in the derived optical constants, but the effect will be lessened in areas where the absorbance is high. It should be pointed out that the problems resulting from nonuniform films may extend to, and may in fact be more severe for, determinations of optical constants using reflection spectra. Previous reflection studies of H_2SO_4 have not considered the possible effects of non-uniform films. Table 1 lists the range of thicknesses and coherences for the films used for each composition studied.

The determination of the optical constants is an iterative process with two steps that are repeated until a converging solution is reached. First, the thickness and coherence of the films are calculated by minimizing the squared difference between the calculated and measured absorbances of the spectra in the region above 4000 cm^{-1} [*Press et al.*, 1989]. For the first time through the iterative loop, the estimated refractive indices are used to calculate the thickness and coherence. After that, the newly calculated refractive indices are used. Second, the refractive indices are adjusted, as described below. This overall sequence is repeated five times.

To adjust the refractive indices, the imaginary refractive index at each frequency is first determined to minimize the squared error between the calculated and measured spectra for all films simultaneously. Then, the values of n at each frequency are calculated using the Kramers-Kronig relationship

$$n(\nu) = n_{vis} + \frac{2\left(\nu^2 - \nu_{vis}^2\right)}{\pi} P \int_0^\infty \frac{k\nu'}{\left(\nu'^2-\nu^2\right)\left(\nu'^2-\nu_{vis}^2\right)} d\nu' \qquad (4)$$

where P indicates that the principal part of the integral is taken, and the subscript vis indicates that values in the visible are used, in our case at 14,000 cm^{-1}. These two steps are repeated five times. Each time, the refractive indices are adjusted unless both the real and imaginary refractive indices change less than 1% from the previous step or the total error between the measured and calculated absorbance spectra drops below 1×10^{-4}. In these cases, the calculation of the refractive indices is terminated at the end of the sequence, and the thickness and coherence are calculated again.

To calculate the Kramers-Kronig integral, some assumptions are necessary. The integral is performed from 0 to 185,800 cm^{-1}. Below 500 cm^{-1} and above 7000 cm^{-1}, it is assumed that the imaginary indices remain constant at the values at 500 and 7000 cm^{-1}, respectively. Above 7000 cm^{-1}, this is a good assumption since little absorption is expected at those frequencies. Because the imaginary indices are very low in this region, the calculation of the Kramers-Kronig integral will not be affected significantly. The assumption of constant imaginary index below 500 cm^{-1}, where the imaginary indices are larger, is not as good. Both assumptions were explored and will be discussed in the section below on errors.

In the step where the imaginary refractive indices are adjusted, it is necessary to minimize the error between the measured and calculated absorbances of the film. In this step, the films were weighted by dividing the error calculated for each film by the maximum absorbance measured for that film. Other

methods of weighting the spectra could be used, one of which is discussed in the section on errors.

Preliminary studies showed that our determination of the imaginary indices was inaccurate above approximately 3650 cm^{-1}. As a result, we did not allow the model to iterate on the imaginary index in this region since this might lead to errors in the calculated film thicknesses. Instead, the imaginary index was assumed to exponentially decay in the same qualitative manner as was measured by *Palmer and Williams* [1975]. This was done by fitting the Palmer and Williams data for all compositions to a curve of the form

$$k(v) = k_{4000}e^{-c\left(v^2 - 4000^2\right)}$$ (5)

where k_{4000} is the average of the imaginary indices at 4000 cm^{-1}. The parameters of the fit were $k_{4000} = 0.0036$ and $c = 1.4086 \times 10^{-7}$. For our analysis, the value of k_{4000} from fitting the spectra was used to calculate the imaginary indices for frequencies above 4000 cm^{-1}, using the same value of c obtained in the fit. Therefore the imaginary indices in the range above 4000 cm^{-1} could slide up and down based on changes in k_{4000}, but always decayed with a constant slope described by equation 5. These imaginary indices were used in the calculations of the real refractive indices using the Kramers-Kronig integral as well as in the iterations on the film thicknesses and coherences.

The visible refractive indices at 14,000 cm^{-1} were calculated using a Lorentz-Lorenz temperature correction of data from *Palmer and Williams* [1975] using equations 2 and 3 . Densities of sulfuric acid solutions measured optically at 221 and 195 K by *Beyer et al.* [1996] were within 1% of the densities calculated by a linear extrapolation from higher-temperature density data. The *Beyer et al.* [1996] study supports the validity of using the Lorentz-Lorenz correction to calculate low-temperature densities and refractive indices in the visible frequency region. Note that in the work of *Toon et al.* [1994], the visible refractive indices were not known and a separate iteration of the Kramers-Kronig program was required to determine them.

4. Optical Constants of H$_2$SO$_4$ Solutions

The optical constants were measured for eight compositions between 45 and 80 wt% H$_2$SO$_4$. In Figure 4, calculated absorption spectra (dotted lines) are compared with the measured spectra (solid lines) for three of these compositions (50, 65, and 75 wt% H$_2$SO$_4$) for a few of the film thicknesses used in the analysis. The relative differences between the spectra are also plotted in each frame over the range 3650-500 cm^{-1}. The calculated and measured spectra match quite well in both the nonabsorbing region above 3700 cm^{-1} and the absorbing regions at lower frequency. With the exception of 45 wt% H$_2$SO$_4$, the comparisons for the other compositions (not shown) are similar to the comparisons for 50, 65, and 75 wt% H$_2$SO$_4$. The spectral matching was poorer for 45 wt% H$_2$SO$_4$, as discussed in the section on errors. The film thicknesses studied ranged from 0.76 μm to 4.08 μm, although in general, the more concentrated films were thinner. The coherence of the films generally decreased as the film thickness increased, and varied between 0.13 and 0.94, although most films had a coherence greater than 0.4. Table 1 lists the range of film thicknesses and coherences for the compositions studied.

The measured optical constants for 45-61 wt% and for 65-80 wt% are reported in Tables 2 and 3, respectively. The real and imaginary indices are only tabulated for a subset of the frequencies for which they were measured. The 120 frequencies reported were chosen to minimize the percent difference between the measured values and values obtained from linear interpolation between the reported values. The maximum and mean percent errors from interpolation are reported in Table 4 for both refractive indices for each composition. Refractive indices at all frequencies measured are available as supporting material through this journal.[1] The optical constants for 50, 65, and 75 wt% H$_2$SO$_4$ solutions are also shown graphically in Figure 5.

The imaginary indices reported in Tables 2 and 3 cover the range 3650-400 cm^{-1}, while the real indices are reported for the range 7000-400 cm^{-1}. The low values of transmittance between 7000 and 3650 cm^{-1} result in unreliable measurements of the imaginary index in this frequency range. To determine the region where measurements of the imaginary index are unreliable, the imaginary indices calculated by two different error weighting methods were compared. The imaginary indices for some compositions were found to differ from the average by more than 5% for frequencies above approximately 3650 cm^{-1}. An analysis of the imaginary refractive indices indicates that the transmittance at the frequency where the difference in these methods becomes large is approximately t=0.8, which is the upper value of transmittance deemed reliable by *Toon et al.* [1994] and *Warren* [1984]. Thus we report the imaginary index only at frequencies where the transmittance is below 0.8. A minimum value for k can be calculated using the equation

$$\Delta t = exp(-4\pi kdv)$$ (6)

where Δt is 0.8, d (cm) is the thickness of the thickest film used in the analysis of a particular composition, and v is the frequency (cm^{-1}). A plot of k_{min} versus frequency is included in Figure 5. From the values of $k_{min}(v)$, we conclude that our imaginary refractive indices are reliable at all frequencies below 3650 cm^{-1}. Although the imaginary indices at frequencies above 3650 cm^{-1} are unreliable, the measured values are low enough so that effects on n (calculated using the Kramers-Kronig relationship) are minimal. This was confirmed by tests of the model, which are described later in the section on errors. Also, as discussed in the previous section, the imaginary indices above 4000 cm^{-1} were constrained in order to prevent artificial effects on the film thicknesses and coherences determined from the spectra in this region.

Our measured refractive indices are compared with refractive indices determined in other studies in Figures 6 and 7. In Figure 6, our values for 75 wt% are compared with the values for 75 wt% measured at 300 K by *Remsberg et al.* [1974], at 300 K by *Palmer and Williams* [1975], and at 250 K by *Pinkley and Williams* [1976]. Figure 7 compares our values for 50 wt% H$_2$SO$_4$ with those measured at 300 K by *Palmer and Williams* [1975].

The overall shapes of our refractive index curves for 75 wt% H$_2$SO$_4$ agree with previous studies. There are, however, large differences in the absolute magnitude of the imaginary indices. For example, for 75 wt% H$_2$SO$_4$, the imaginary indices we measured are higher than those measured by both *Palmer and Williams* [1975] and *Pinkley and Williams* [1976], by nearly a factor of 2 between 700 and 800 cm^{-1}. On average, our imaginary index values for the complete frequency range of each study were 1.04, 1.31, and 1.45 times larger than those of
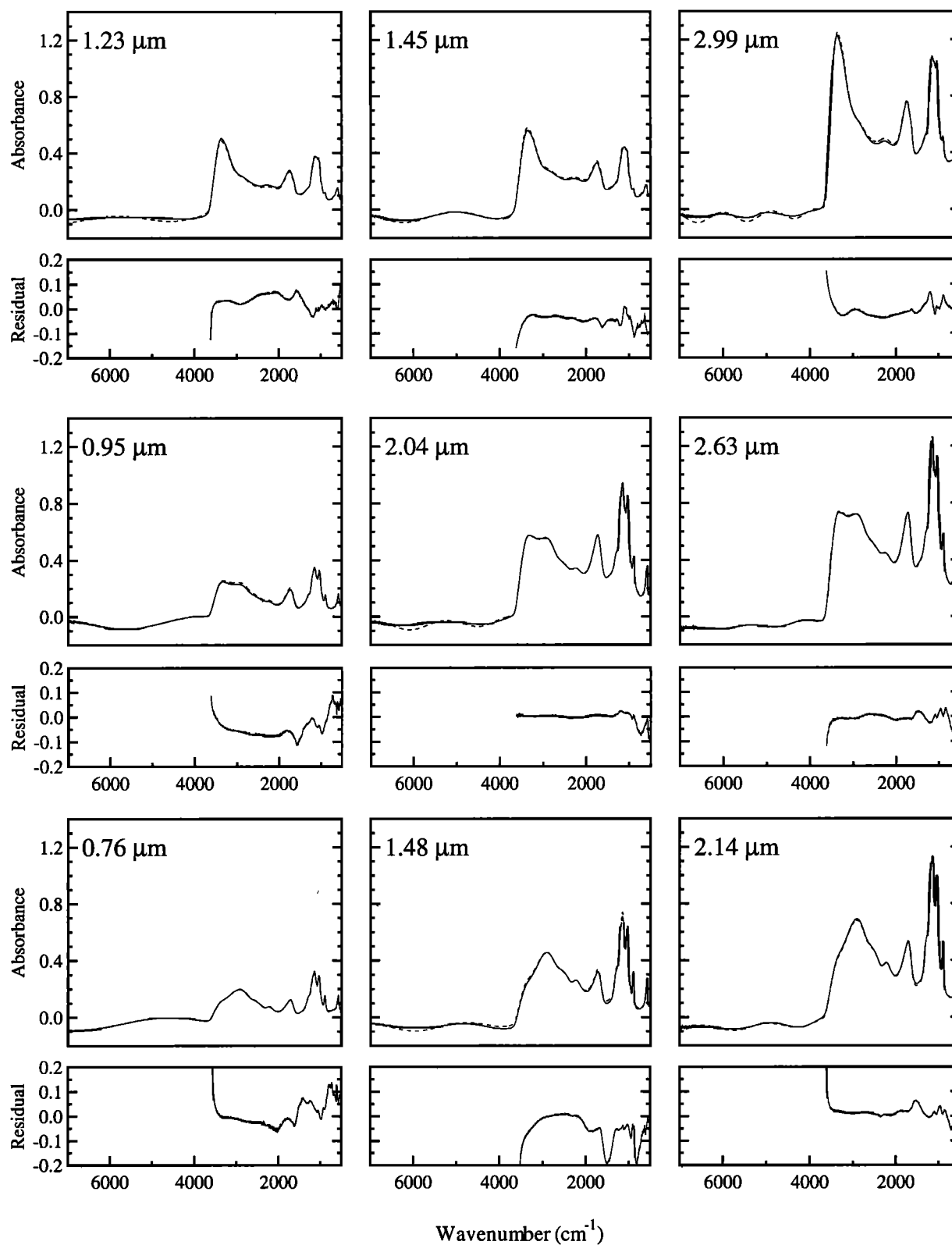
Figure 4. Observed absorption spectra of (top) 50, (middle) 65, and (bottom) 75 wt% H_2SO_4 films (solid lines) and a theoretical spectrum (dots) based on the optical constants in Tables 2 and 3. The curve in the lower box for each frame is the residual of the two absorbances, calculated as (observed-theoretical)/(observed). The film thickness for each spectrum is plotted in the upper left corner of the frame.

Table 2. Optical Constants of 45.2, 50.0, 55.1, and 61.6 wt% H_2SO_4 Solutions

cm^{-1}	45.2 wt%		50.0 wt%		55.1 wt%		61.6 wt%	
	n	k	n	k	n	k	n	k
499.5	1.989	0.400	2.013	0.421	2.032	0.435	2.067	0.426
503.3	1.887	0.403	1.905	0.426	1.920	0.440	1.958	0.429
511.1	1.835	0.404	1.848	0.422	1.861	0.437	1.903	0.428
514.9	1.827	0.405	1.840	0.425	1.853	0.438	1.895	0.428
538.1	1.812	0.416	1.828	0.434	1.842	0.448	1.897	0.442
549.6	1.813	0.425	1.832	0.445	1.848	0.460	1.912	0.460
553.5	1.814	0.430	1.834	0.450	1.854	0.461	1.920	0.470
561.2	1.816	0.440	1.842	0.465	1.864	0.487	1.935	0.508
568.9	1.820	0.459	1.846	0.498	1.869	0.534	1.932	0.579
572.8	1.819	0.472	1.842	0.519	1.859	0.563	1.911	0.621
576.6	1.816	0.486	1.831	0.541	1.838	0.590	1.874	0.654
584.4	1.802	0.513	1.795	0.575	1.785	0.618	1.793	0.669
592.1	1.780	0.539	1.754	0.591	1.730	0.625	1.727	0.656
607.5	1.705	0.574	1.657	0.594	1.627	0.599	1.623	0.604
622.9	1.627	0.541	1.589	0.533	1.571	0.520	1.575	0.507
626.8	1.617	0.529	1.583	0.514	1.569	0.500	1.577	0.482
642.2	1.583	0.478	1.564	0.457	1.559	0.441	1.584	0.423
653.8	1.581	0.449	1.568	0.423	1.569	0.407	1.599	0.391
673.1	1.585	0.421	1.583	0.391	1.591	0.375	1.625	0.359
700 1	1.583	0.400	1.595	0.367	1.612	0.350	1.653	0.339
773.4	1 569	0.349	1.613	0.322	1.644	0.316	1.701	0.314
792.7	1.572	0.335	1.624	0.311	1.657	0.309	1.718	0.312
796.6	1.573	0.332	1.627	0.311	1.661	0.309	1.722	0.312
819.7	1.581	0.318	1.643	0.304	1.680	0.306	1.744	0.315
823.6	1.583	0.315	1.647	0.302	1.685	0.306	1.749	0.317
839.0	1.593	0.308	1.663	0.304	1.703	0.312	1.771	0.326
854.4	1.606	0.305	1.680	0.311	1.724	0.325	1.796	0.346
866.0	1.617	0.308	1.693	0.323	1.738	0.344	1.813	0.373
873.7	1.622	0.312	1.699	0.335	1.742	0.364	1.819	0.401
881.4	1.626	0.317	1.699	0.351	1.738	0.384	1.812	0.435
889.2	1.628	0.322	1.693	0.364	1.725	0.404	1.789	0.465
896.9	1.626	0.327	1.682	0.372	1.706	0.412	1.757	0 477
900.7	1.625	0.328	1.676	0 371	1 696	0.412	1.740	0.475
904.6	1.624	0 327	1 671	0.370	1.687	0.408	1.725	0.470
908.4	1.624	0 325	1.668	0.366	1.680	0.402	1 713	0.461
923.9	1.633	0.318	1.673	0.349	1.681	0.375	1.707	0.413
931 6	1.642	0.317	1.683	0.347	1.693	0.367	1.721	0.399
939.3	1.653	0.319	1.696	0.348	1.709	0.366	1.741	0.396
947 0	1.665	0.325	1.711	0.354	1.724	0.373	1.760	0.402
958.6	1.680	0.342	1.729	0.374	1.745	0.391	1.784	0.422
970.2	1.689	0.367	1.740	0.403	1.756	0.420	1.799	0.452
985.6	1.680	0.386	1.733	0.430	1.754	0.453	1.802	0.490
989 5	1.685	0.381	1.736	0.431	1.756	0.456	1.804	0.496
997.2	1.705	0.395	1.753	0.447	1.771	0.473	1.817	0.518
1008.8	1.719	0.439	1.760	0.499	1.776	0.528	1.820	0.577
1028.0	1.699	0.517	1.721	0.586	1.728	0.616	1.764	0.679
1043.5	1.653	0.570	1.654	0.632	1.649	0.664	1.667	0.723
1055.1	1.605	0.586	1 589	0.638	1.580	0.656	1.589	0.707
1070.5	1.564	0.593	1.555	0.615	1.542	0.616	1.547	0.648
1085.9	1.517	0.611	1.523	0.621	1.528	0.609	1.548	0.627
1101.3	1.456	0.621	1.478	0.621	1.501	0.610	1.541	0.632
1109.1	1.424	0.613	1.455	0.615	1.489	0.612	1.535	0.639
1132.2	1.343	0.574	1.404	0.604	1.446	0.618	1.499	0.674
1147.6	1.300	0.536	1.363	0.592	1.405	0.624	1.443	0.702
1166.9	1.262	0.476	1.302	0.564	1.328	0.612	1.346	0.691
1193.9	1.248	0.398	1.247	0.483	1.254	0.536	1.255	0.608
1217.1	1.250	0.349	1.226	0.421	1.216	0.466	1.203	0.534
1236.4	1.257	0.306	1.221	0.360	1.204	0.395	1.181	0.451
1248.0	1.269	0.284	1.232	0.323	1.213	0.352	1.189	0.403
1259.5	1.282	0.268	1.249	0.297	1.231	0.320	1.208	0.365
1271.1	1.295	0.256	1.268	0.281	1.253	0.300	1.231	0.340
1282.7	1.306	0.249	1.284	0.270	1.271	0.288	1.251	0.328
1302.0	1.320	0.240	1.304	0.260	1.291	0.277	1.268	0.317
1321.3	1.330	0.231	1.315	0.253	1.301	0.268	1.274	0.302
1348.3	1.340	0.221	1.325	0.239	1.311	0.249	1.283	0.271
1363.7	1.346	0.214	1.331	0.230	1.319	0.238	1.294	0.256
1398.4	1.360	0.202	1.348	0.213	1.339	0.219	1.320	0.230
1456.3	1.381	0.187	1.374	0.195	1.367	0.198	1.355	0.206
1521.9	1.408	0.177	1.407	0.182	1.402	0.182	1.394	0.187
1541.2	1.419	0.175	1.419	0.181	1.415	0.179	1.409	0.184
1579.8	1.444	0.185	1.447	0.188	1.446	0.186	1.442	0.189
1595.2	1.453	0.194	1.459	0.198	1.458	0.196	1.456	0.198
1618.3	1.461	0.218	1.469	0.222	1.470	0.219	1.470	0.219
1637.6	1.453	0.239	1.464	0.243	1.469	0.238	1.473	0.241
1672.4	1 427	0.255	1.447	0.266	1.455	0.267	1.463	0 278
1707.1	1.408	0.263	1.424	0.286	1.430	0.291	1.430	0.308
1726.4	1.393	0.267	1.405	0.292	1.407	0.298	1.404	0.311

Table 2. (continued)

cm^{-1}	45.2 wt%		50.0 wt%		55.1 wt%		61.6 wt%	
	n	k	n	k	n	k	n	k
1757.2	1.367	0.261	1.372	0.287	1.374	0.291	1.368	0.300
1815.1	1.336	0.229	1.336	0.252	1.336	0.254	1.332	0.258
1869.1	1.327	0.195	1.324	0.215	1.326	0.216	1.325	0.217
1930.8	1.334	0.164	1.331	0.181	1.334	0.181	1.335	0.181
1988.7	1.348	0.147	1.345	0.162	1.349	0.162	1.353	0.162
2054.3	1.362	0.140	1.359	0.153	1.364	0.153	1.371	0.153
2146.9	1.371	0.136	1.370	0.149	1.377	0.150	1.387	0.153
2197.1	1.373	0.134	1.372	0.148	1.380	0.151	1.390	0.156
2270.4	1.374	0.130	1.372	0.145	1.379	0.149	1.388	0.155
2332.1	1.375	0.124	1.372	0.139	1.379	0.144	1.389	0.149
2397.7	1.379	0.117	1.375	0.132	1.383	0.138	1.395	0.146
2548.1	1.396	0.109	1.389	0.127	1.392	0.137	1.400	0.151
2679.3	1.409	0.116	1.396	0.132	1.396	0.141	1.401	0.156
2845.2	1.417	0.128	1.396	0.143	1.389	0.154	1.386	0.174
2976.4	1.429	0.143	1.395	0.150	1 381	0.156	1.365	0.172
3026.6	1.434	0.155	1.397	0.155	1.379	0.157	1.359	0.169
3092.1	1.438	0.181	1.398	0.170	1.378	0.164	1.354	0.167
3242.6	1.384	0.260	1.361	0.220	1.350	0.195	1.332	0.174
3350.6	1.293	0.280	1.294	0.235	1.299	0.206	1.296	0.176
3396.9	1.241	0.269	1.253	0.227	1.266	0.198	1.272	0.168
3443.2	1.194	0.236	1.215	0.201	1.234	0.176	1.249	0.149
3485.7	1.163	0.191	1.191	0.164	1.214	0.146	1.235	0.124
3489.5	1.161	0.186	1.189	0.161	1.213	0.143	1.234	0.122
3493.4	1.159	0.182	1.187	0.157	1.211	0.139	1.233	0.119
3497.2	1.158	0.177	1.186	0.154	1.210	0.136	1.232	0.117
3539.7	1.149	0.125	1.178	0.111	1.203	0.100	1.227	0.087
3547.4	1.150	0.115	1.178	0.103	1.203	0.093	1.227	0.081
3586.0	1.161	0.071	1.185	0.065	1.209	0.061	1.233	0.054
3593.7	1.164	0.063	1.188	0.058	1.212	0.054	1.235	0.049
3609 1	1.173	0.049	1.195	0.045	1.218	0.042	1.241	0.039
3620.7	1.181	0.040	1.201	0.036	1.224	0.035	1.246	0.032
3632.3	1.189	0.031	1.208	0.029	1.230	0.028	1.252	0.026
3647.7	1.200	0.023	1.218	0.020	1.239	0.021	1.260	0.020
3701.7	1.236		1.251		1.268		1.285	
3802.0	1.275		1.286		1.299		1.311	
3902.3	1.297		1.306		1.316		1.327	
3998.8	1.311		1.319		1.328		1.338	
4500.4	1.348		1.355		1.362		1.369	
5001.9	1.366		1.372		1.379		1.386	
5499.6	1.377		1.383		1.389		1.397	
6001.2	1.384		1.390		1.397		1.404	
6498.9	1.389		1.395		1.402		1.409	
6996.6	1.393		1.399		1.406		1.413	

Remsberg et al.[1974], *Palmer and Williams*[1975], and *Pinkley and Williams* [1976], respectively. This indicates that our data matches the data of Remsberg et al. more closely than the other studies. However, it should be noted that for the limited frequency range of *Remsberg et al.* [1974] our values averaged only 1.27 and 1.34 times larger than those of *Palmer and Williams* [1975] and *Pinkley and Williams* [1976], respectively. As can be seen from a comparison of the optical constants at three different temperatures for 75 wt% H$_2$SO$_4$ (Figure 6), a linear interpolation between *Palmer and Williams'* [1975] 300 K data and our 215 K data will not give an accurate estimate of *Pinkley and Williams'* [1976] 250 K data, so we did not attempt such an interpolation.

For 50 wt% H$_2$SO$_4$, there are significant qualitative differences between our refractive indices and those of *Palmer and Williams* [1975], and the quantitative differences remain. The region where our 215 K indices qualitatively differ most is the region between 1000 and 1200 cm^{-1}, where there are two peaks in the imaginary index at 300 K. At 215 K, these peaks appear to have coalesced into one peak, a phenomenon which has been observed previously in low-temperature infrared studies of H$_2$SO$_4$ [*Middlebrook et al.* 1993; *Anthony et al.*, 1995;

Clapp et al., 1997]. As a result of this peak coalescence, our measured imaginary index at 1070 cm^{-1} is about twice as large as that measured by *Palmer and Williams* [1975] for 50 wt%. On average, our imaginary indices for 50 wt% H$_2$SO$_4$ are 1.55 times larger than those measured by *Palmer and Williams* [1975].

Note that a satellite-retrieved absorption optical depth in the Rayleigh limit is directly proportional to the product of the imaginary refractive index and the aerosol mass. Therefore an underestimate of the imaginary refractive index will result in an overestimate of the aerosol mass. This implies that studies using the reflection-derived room temperature optical constants may have overestimated the aerosol mass by as much as a factor of 2 depending on the frequencies used.

There are two possible reasons for the differences in our optical constants from those measured in previous studies. There may be a real temperature dependence in the refractive indices. Also, there may be errors in the previous measurements. A combination of these reasons is likely to explain the differences between our study and previous studies. *Palmer and Williams* [1975] and *Pinkley and Williams* [1976] measured their refractive indices using a reflection technique. In a dis-

Table 3. Optical Constants of 65.3, 70.2, 75.0, and 80.0 wt% H_2SO_4 Solutions

	65.3 wt%		70.2 wt%		75.0 wt%		80.0 wt%	
cm^{-1}	n	k	n	k	n	k	n	k
499.5	2.098	0.418	2.100	0.397	2.103	0.366	2.089	0.338
503.3	1.992	0.425	2.000	0.402	2.013	0.366	2.005	0.340
511.1	1.937	0.423	1.950	0.399	1.971	0.366	1.970	0.335
514.9	1.931	0.421	1.946	0.398	1.969	0.364	1.970	0.335
538 1	1.940	0.438	1.968	0.416	2.006	0.387	2 021	0.363
549.6	1.963	0.462	1.999	0.448	2.053	0.428	2.079	0 413
553.5	1.973	0.477	2 015	0.466	2 071	0.454	2.102	0 446
561.2	1.994	0.525	2 041	0.534	2.104	0.546	2 128	0.571
568.9	1.986	0.617	2.017	0.656	2.052	0.703	2 038	0.738
572.8	1.953	0.667	1.968	0 711	1.981	0.756	1.953	0.775
576.6	1.905	0.697	1.903	0.738	1.903	0.769	1.871	0.776
584 4	1.809	0.707	1.792	0.726	1.784	0.740	1.753	0.727
592.1	1.738	0.687	1.715	0.690	1.707	0.689	1.684	0.669
607.5	1.630	0.622	1.615	0.603	1.613	0.593	1.604	0 570
622.9	1.581	0.512	1.575	0.489	1.575	0.470	1.566	0.451
626.8	1.584	0.485	1.581	0.459	1.583	0.439	1 574	0.414
642.2	1.595	0.419	1.601	0.394	1.612	0.373	1 611	0.350
653.8	1.615	0.386	1 625	0.365	1.638	0.346	1.639	0.328
673.1	1.646	0.355	1.657	0.335	1.673	0.318	1.669	0.308
700.1	1.677	0.333	1.692	0.314	1.708	0.301	1.700	0.289
773.4	1.736	0.311	1.755	0 297	1.766	0.282	1 748	0.254
792.7	1.755	0.311	1.774	0 296	1 786	0.277	1.766	0.250
796.6	1.759	0.311	1.779	0 295	1.792	0.275	1.772	0.239
819.7	1.784	0.316	1.808	0 299	1.825	0.275	1.810	0.240
823 6	1.789	0.317	1.814	0 301	1 832	0.276	1.820	0.231
839.0	1.815	0 326	1.844	0 311	1.866	0.284	1.862	0.238
854.4	1.846	0 348	1.880	0 334	1.910	0.306	1.914	0 259
866.0	1.867	0.382	1.909	0.371	1.948	0.343	1.961	0.293
873 7	1.876	0.416	1.922	0.409	1 970	0.386	1.992	0.337
881 4	1.868	0.454	1.920	0.462	1.976	0.448	2.011	0 409
889.2	1.845	0.493	1.892	0.514	1 950	0 517	1 989	0.494
896.9	1.805	0.515	1.838	0.547	1.887	0.568	1 923	0.563
900 7	1.781	0.515	1.808	0.549	1 848	0.576	1 878	0 581
904.6	1.761	0.506	1.779	0.543	1 810	0 573	1 831	0 584
908 4	1.746	0 494	1.754	0.528	1 775	0 558	1 786	0 573
923.9	1.734	0.434	1 726	0 438	1.721	0.444	1.695	0 441
931.6	1.752	0.416	1.750	0.408	1.746	0.395	1.716	0.372
939.3	1.774	0.411	1.780	0.397	1.785	0.375	1 762	0.337
947.0	1.796	0.417	1 809	0.401	1 823	0.373	1.808	0.325
958.6	1.825	0.436	1 845	0.421	1.869	0.393	1.867	0 341
970.2	1.844	0 468	1.870	0.455	1 903	0.427	1.912	0.369
985.6	1.850	0.513	1.888	0.504	1 935	0.478	1.965	0 421
989 5	1.854	0.519	1.892	0 515	1 944	0.490	1.978	0 439
997 2	1.869	0.546	1.907	0.543	1 965	0.525	2.007	0 480
1008.8	1.872	0.612	1.917	0.618	1 983	0.611	2 033	0.581
1028.0	1.813	0.728	1.853	0.756	1.914	0.780	1 958	0.775
1043.5	1 700	0.783	1.723	0.817	1.764	0.851	1.793	0.857
1055.1	1.611	0.761	1 622	0.788	1.651	0.825	1.671	0.826
1070 5	1.563	0.690	1 567	0.704	1.584	0.721	1 599	0.715
1085.9	1.571	0.663	1.588	0.659	1.618	0.664	1.647	0.649
1101.3	1.574	0 670	1.607	0.672	1.656	0.689	1.698	0.689
1109.1	1.571	0.681	1.612	0.693	1.661	0.718	1.704	0.734
1132.2	1.531	0.737	1.567	0.777	1.599	0.834	1 607	0.872
1147.6	1.463	0.773	1.479	0.822	1.493	0.877	1.481	0.897
1166.9	1.348	0.761	1.355	0.801	1.356	0.847	1.346	0.850
1193.9	1.244	0.672	1.239	0.714	1.231	0.757	1.227	0.762
1217.1	1.181	0.587	1.166	0.620	1 145	0.660	1 138	0.663
1236 4	1.156	0.494	1.137	0.518	1.114	0.547	1.105	0.549
1248 0	1.165	0.440	1.147	0.460	1.122	0.486	1.113	0.489
1259 5	1.185	0.397	1.168	0.419	1.144	0.441	1.133	0.446
1271 1	1.210	0.371	1.191	0.393	1.166	0.416	1.149	0.420
1282.7	1.229	0.358	1.209	0.379	1.179	0.402	1.155	0.405
1302.0	1.245	0.345	1.217	0.362	1.178	0.377	1.147	0.372
1321.3	1.247	0.325	1.213	0.333	1.172	0.333	1.139	0.314
1348.3	1.259	0.283	1.227	0.277	1.193	0.261	1 169	0.227
1363.7	1.272	0.264	1.246	0.251	1.217	0.231	1.201	0.193
1398.4	1.305	0.235	1.288	0.219	1.273	0.194	1 268	0.154
1456.3	1.346	0.210	1.340	0.193	1.337	0.169	1 346	0.133
1521.9	1.391	0.190	1.392	0.175	1.397	0.155	1.411	0.126
1541.2	1.407	0.186	1.409	0.173	1.415	0.155	1.429	0.128
1579.8	1.443	0 193	1.446	0.181	1.452	0.164	1.466	0.142
1595.2	1.457	0.201	1 460	0.189	1.467	0.173	1 479	0 152
1618.3	1.473	0.223	1 478	0.211	1.485	0.196	1 494	0.174
1637.6	1.479	0.247	1.485	0.235	1.491	0.221	1.499	0.199
1672.4	1.469	0.288	1.472	0.283	1.477	0.267	1.479	0.236
1707.1	1.429	0.320	1.429	0.312	1.435	0.289	1.445	0.248
1726.4	1.401	0.322	1 401	0.310	1.409	0.288	1.428	0.243

Table 3. (continued)

cm^{-1}	65.3 wt%		70.2 wt%		75.0 wt%		80.0 wt%	
	n	k	n	k	n	k	n	k
1757.2	1.364	0.309	1.366	0.293	1.380	0.268	1.409	0.228
1815.1	1.329	0.262	1.337	0.245	1.360	0.224	1.399	0.195
1869.1	1 324	0.220	1.337	0.204	1.364	0.190	1.406	0.171
1930.8	1.337	0.183	1.353	0.173	1.381	0.164	1.422	0.154
1988.7	1.356	0.164	1.373	0.157	1.401	0.151	1.441	0.147
2054.3	1.375	0.155	1.393	0.151	1.422	0.150	1.460	0.153
2146.9	1.393	0.158	1 409	0.159	1.436	0.166	1.471	0.176
2197.1	1.395	0.162	1.409	0.165	1.431	0.174	1.459	0.192
2270.4	1.392	0.160	1.404	0.160	1.421	0.168	1.439	0.181
2332.1	1.395	0.154	1.408	0.154	1.428	0.159	1.450	0.167
2397.7	1 402	0.152	1.417	0.155	1.439	0.165	1.462	0.181
2548.1	1.405	0.160	1.415	0.168	1.430	0.186	1.445	0.208
2679.3	1.405	0.167	1.413	0.175	1.421	0.192	1.427	0.217
2845.2	1.386	0.188	1.388	0.200	1.387	0.219	1.379	0.239
2976.4	1.357	0.185	1.350	0.194	1.340	0.208	1.323	0.220
3026.6	1.349	0.180	1.338	0.187	1.326	0.198	1.308	0.204
3092.1	1.341	0.174	1.325	0.175	1.310	0.181	1.291	0.180
3242.6	1.319	0.169	1.306	0.153	1.294	0.141	1.279	0.126
3350.6	1.289	0.165	1.287	0.140	1.284	0.119	1.281	0.095
3396.9	1.269	0.155	1.274	0.130	1.277	0.108	1.281	0.084
3443.2	1.249	0.137	1.261	0.113	1.272	0.092	1.282	0.069
3485.7	1.238	0.112	1.255	0.093	1.270	0.076	1.287	0.055
3489.5	1.238	0.110	1.254	0.091	1.269	0.074	1.286	0.057
3493.4	1.237	0.108	1.254	0.089	1.269	0.072	1.287	0.053
3497.2	1.236	0.105	1.253	0.087	1.269	0.071	1.287	0.054
3539.7	1.234	0.078	1.253	0.064	1.272	0.052	1.291	0.040
3547.4	1.234	0.073	1.254	0.060	1.273	0.049	1.291	0.036
3586.0	1.240	0.048	1.261	0.038	1.280	0.033	1.299	0.027
3593.7	1.243	0.043	1.263	0.035	1.282	0.030	1.301	0.023
3609.1	1.248	0.034	1.268	0.027	1.287	0.024	1.306	0.019
3620.7	1.253	0.028	1.273	0.022	1.291	0.020	1.310	0.016
3632.3	1.259	0.023	1.278	0.018	1.295	0.017	1.314	0.014
3647.7	1.266	0.018	1.285	0.014	1.301	0.014	1.319	0.012
3701.7	1.290		1.305		1.319		1.332	
3802.0	1.316		1.329		1.339		1.348	
3902 3	1 332		1.343		1.352		1 360	
3998.8	1.343		1.353		1.361		1.369	
4500.4	1.374		1.383		1.391		1.398	
5001.9	1.391		1.400		1.407		1.413	
5499 6	1.402		1 410		1.417		1.423	
6001.2	1.409		1.417		1.425		1.430	
6498.9	1.415		1.422		1.430		1.436	
6996.6	1.419		1.426		1.434		1.439	

cussion of their errors, *Palmer and Williams* [1975, p. 215] mention that over most of the measurement range of *Remsberg et al.* [1974], their values agree within their uncertainty, and that "greater precision is usually claimed for ATR results than we claim for results based upon measurements of reflectance at a free liquid surface."

Part of the difference between our measured optical constants and those of *Palmer and Williams* [1975] and *Pinkley and Williams* [1976] results from the difference in temperature of the measurements. For example, observed shifts in the wavelengths of the absorption maxima, most notably the coalescence of the two sulfate peaks to one peak for dilute solutions

Table 4. Estimated Errors From Composition Fits and Frequency Interpolations

Nominal wt%	Percent Error From Composition Fit				Percent Error From Frequency Interpolation			
	Mean		Maximum		Mean		Maximum	
	n	k	n	k	n	k	n	k
45.2	0.1	0.6	0.6	3.1	0.1	0.5	1.0	2.0
50.0	0.1	1.3	1.0	6.4	0.1	0.4	0.7	1.9
55.1	0.1	0.9	0.5	2.1	0.1	0.4	0.7	1.4
61.6	0.1	0.8	0.7	8.1	0.1	0.4	0.6	1.5
65.3	0.1	1.5	0.6	2.6	0.1	0.4	0.7	1.5
70.2	0.1	0.8	0.4	12.3	0.1	0.5	0.8	1.7
75.0	0.1	0.7	0.6	2.7	0.1	0.6	1.1	2.2
80.0	0.1	0.5	0.3	2.9	0.1	0.7	1.2	2.7
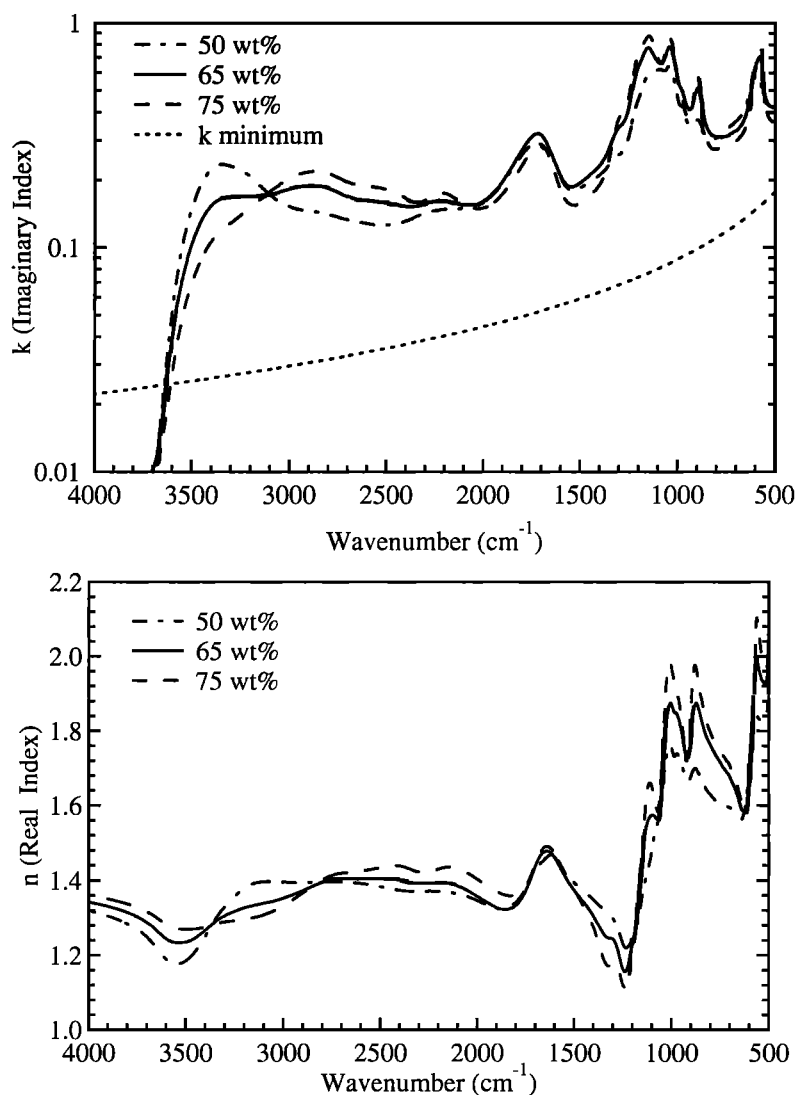
Figure 5. Our measured imaginary and real refractive indices for 50, 65, and 75 wt% H$_2$SO$_4$ solutions at 215 K. The k minimum curve in the plot of the imaginary refractive indices represents our estimate of the smallest value of the imaginary index that could be measured accurately for the film thicknesses we were able to grow.

at low temperatures, are due to temperature dependences [*Middlebrook et al.*, 1993; *Anthony et al.*, 1995; *Clapp et al.*, 1997]. Part of the difference also must be due to errors in one or more of the studies since our measured indices and *Palmer and Williams'* [1975] indices at 300 K do not interpolate to give *Pinkley and Williams'* [1976] indices at 250 K for 75 wt% H$_2$SO$_4$. Because our indices agree more closely with the indices of *Remsberg et al.* [1974], we believe that there are errors in the reflection technique used by *Palmer and Williams* [1975] and *Pinkley and Williams* [1976], especially at frequencies where the imaginary indices, and therefore the reflectance, is low. These errors at low imaginary index are reflected by the error estimates of *Palmer and Williams* [1975], given as $\delta k = \pm 0.03$ independent of the magnitude of k. Unfortunately, without additional studies where the optical constants are measured at low and high temperatures with the same technique, it may be impossible to determine how much of the difference between the various optical constants is real and how much results from errors in one or more studies.

5. Interpolation Scheme for Intermediate Compositions

In order to allow the estimation of the optical constants for any composition in our measurement range, we have created an interpolation scheme. Fits to the optical constants were performed as a function of concentration at each frequency where the indices were measured. The fits were third-order polynomials of the form

$$n[wt] = p_3[wt]^3 + p_2[wt]^2 + p_1[wt] + p_0 \qquad (7)$$

$$k[wt] = q_3[wt]^3 + q_2[wt]^2 + q_1[wt] + q_0 \qquad (8)$$

where wt is the wt fraction H$_2$SO$_4$, given as 0.45, 0.50, etc.

The fit parameters are reported in Table 5 for the same frequencies listed in Tables 2 and 3. The fits for k are shown in Figure 8 for a few frequencies corresponding to various peaks in the spectra of H$_2$SO$_4$ solutions.
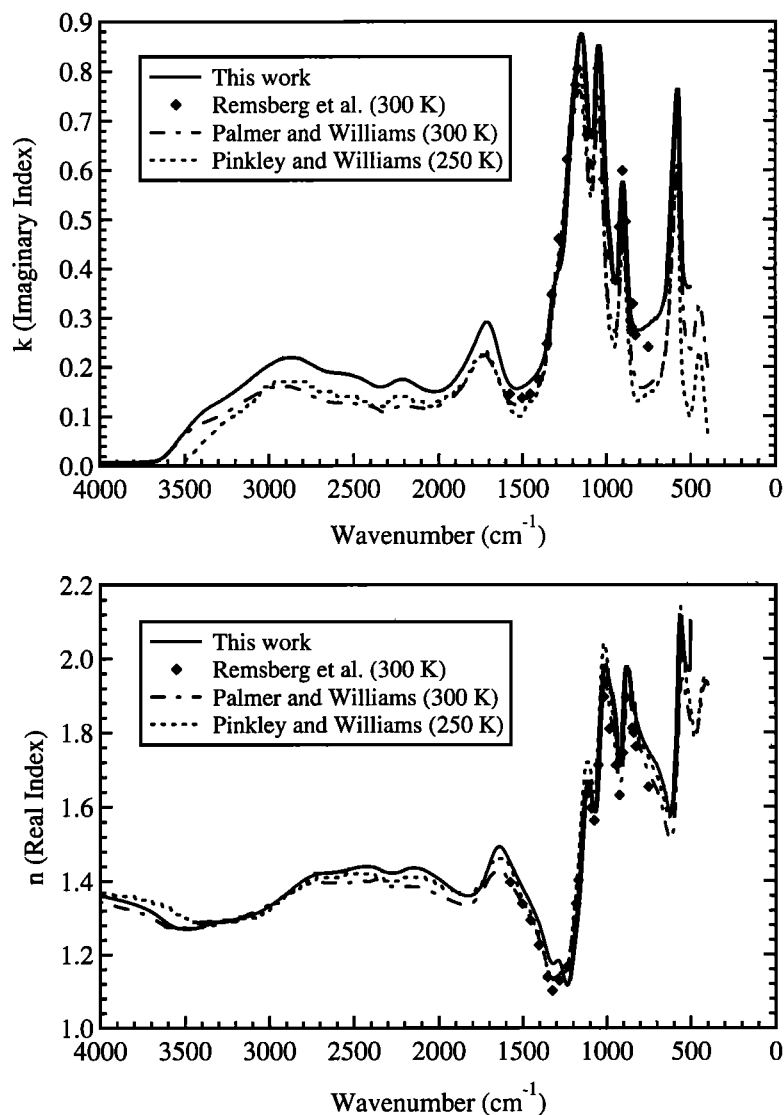
Figure 6. The imaginary and real refractive indices of 75 wt% H_2SO_4 measured in this work at 215 K, measured by *Remsberg et al.* [1974] and *Palmer and Williams* [1975] at 300 K, and by *Pinkley and Williams* [1976] at 250 K.

It can be seen that the peaks at 1051, 1151, and 2880 cm^{-1} increase in intensity as the wt% H_2SO_4 increases, consistent with their assignments as bands from HSO_4^- ions and H_2SO_4 molecules [*Querry et al.*, 1974; *Guldan et al.*, 1995]. In contrast, the peak at 3351 cm^{-1} increases with decreasing wt% H_2SO_4, which agrees with its assignment as the OH stretch of H_2O [*Querry et al.*, 1974; *Guldan et al.*, 1995]. The peak at 1723 cm^{-1} has a maximum in the center of the composition range, consistent with its assignment as the v_4 band in H_3O^+ ions [*Querry et al.*, 1974].

We consider these fits to represent a measure of the precision of our measurement technique and believe that the fits will smooth out any bias toward higher or lower imaginary indices for each individual composition due to film thickness or temperature uncertainties. As a result, we recommend that the fit parameters be used to calculate the optical constants for a particular composition rather than interpolations between the measured data. This will be discussed further in the next section.

6. Errors and Model Testing

We have attempted to examine our known sources of error where possible. It should be pointed out that there may be other unconsidered sources of error we have not examined here. However, the estimation of errors in our measured optical constants was done in several ways, and we believe that we have discussed the largest sources of error in our measurements.

The most significant sources of error are the assumptions that all the spectra used in the analysis of each composition are at the same composition and temperature, and that the coherences and thicknesses are exactly known. To estimate this error, the imaginary indices needed to obtain a perfect fit to the data were calculated for each film used in the analysis. The percent difference in k for the film requiring the maximum adjustment in k was calculated for each frequency. Then, to estimate the error in the real index, the real indices were recalculated from the "perfect fit" imaginary indices using the Kramers-Kronig integral. The means and maxima of these percent differ-
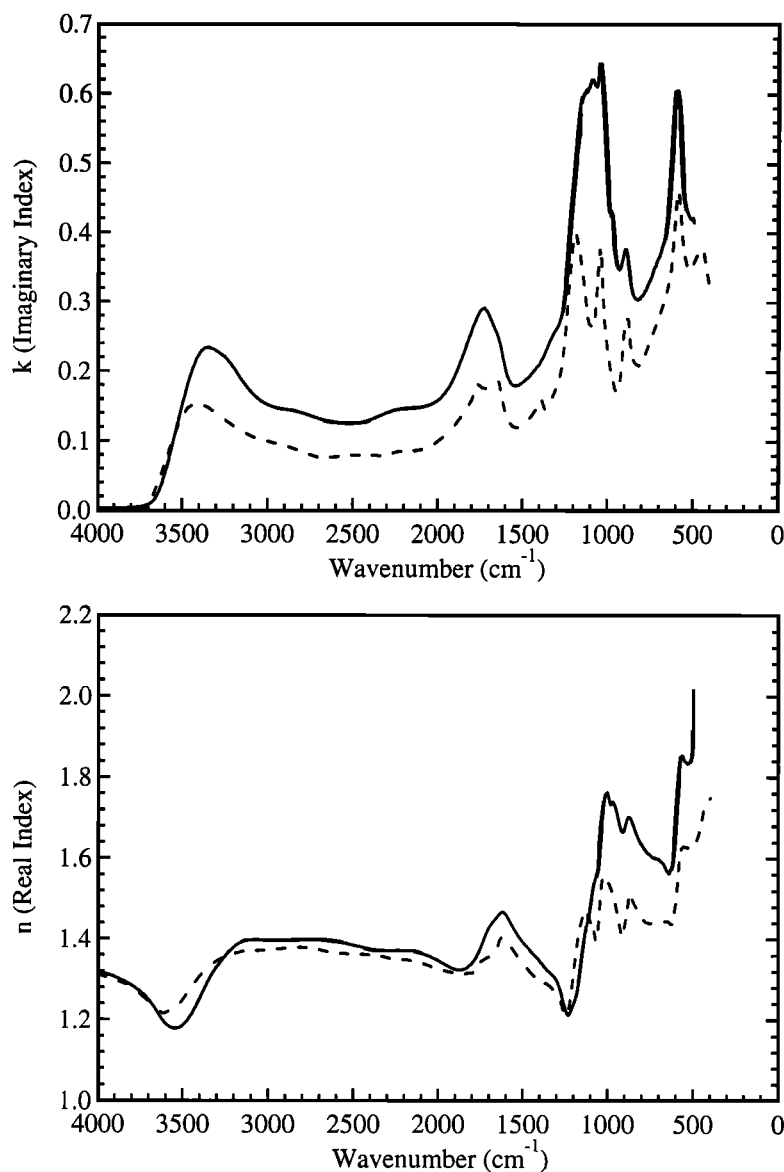
Figure 7. The imaginary and real refractive indices of 50 wt% H_2SO_4 at 215 K (this work, solid lines) and at 300 K (*Palmer and Williams* [1975], dashed lines).

ences, which are due to the mismatch of the measured and calculated spectra in the indices, are reported for each composition in Table 6. In Figure 9, the percent differences in the indices for 75 wt% H_2SO_4 are shown as a function of frequency. This plot illustrates that the rather high maximum errors reported for the imaginary index are misleading in that the maximum errors generally fall in the range between 3500 and 3650 cm^{-1}. If frequencies above 3500 cm^{-1} are disregarded, the maximum error is less than 6.5% for all compositions except one. The exception is 45.2 wt% H_2SO_4, which has a maximum error of 10% below 3500 cm^{-1}.

Errors resulting from assumptions made in the model were tested by changing the optical constant iteration program. It should be noted that the assumptions were changed in these tests, but we cannot say whether the test assumptions are better than the assumptions made in the analysis. However, the tests are used to further characterize our possible errors.

The first model test was to compare results obtained by scaling the difference in absorbance between model and experiment by the maximum absorbance (the normal method of analysis) with those obtained by using the absolute difference in absorbance. The mean and maximum percent differences between these two methods are reported in Table 6. Note that the mean percent differences are lower than the differences from the spectral mismatch tests discussed above.

A second test examined the effects of assuming that the imaginary index is constant below 500 cm^{-1}. In this test, the imaginary index was instead assumed to extrapolate linearly to 0 at 0 cm^{-1}. The percent difference in the indices for these two scenarios is shown in Figure 9. It can be seen that the maximum estimated error in the imaginary index from this assumption is less than 2.2% over the full frequency range. The next model test looked at the effects of the assumptions made for the imaginary index above 3650 cm^{-1}. Instead of a exponential de-

Table 5. Fit Parameters for n and k

cm^{-1}	Parameters for n Using Equation 7				Parameters for k Using Equation 8			
	p_3	p_2	p_1	p_0	q_3	q_2	q_1	q_0
499.5	-6.71971	11.38330	-5.86700	2.93678	2.86867	-7.27306	5.46773	-0.85119
503.3	-7.94224	14.20400	-7.87199	3.27804	2.78385	-7.20665	5.47926	-0.85865
511.1	-7.60649	13.98080	-7.94156	3.27071	2.33578	-6.37064	4.96435	-0.75608
514.9	-8.56518	15.89400	-9.16404	3.51435	2.39134	-6.42764	4.95951	-0.74494
538.1	-9.39795	17.95750	-10.55450	3.78386	2.19464	-5.89014	4.57424	-0.65219
549.6	-9.08943	17.79770	-10.55730	3.78988	1.73733	-4.70719	3.76174	-0.47481
553.5	-9.04499	17.80600	-10.55720	3.78489	1.97783	-4.87750	3.77252	-0.46351
561.2	-10.32610	20.10960	-11.82320	4.00763	2.70047	-5.34208	3.80575	-0.43898
568 9	-14.04750	25.77700	-14.70560	4.50105	3.04297	-5.49445	4.04081	-0.52921
572.8	-14.46880	25.97620	-14.70200	4.49796	-5.10077	9.18415	-4.47709	1.09345
576.6	-10.98460	19.35240	-10.83160	3.77470	-5.87856	9.83179	-4.38902	1.00680
584.4	-8.61623	15.54400	-9.22080	3.59173	-4.16083	5.77754	-1.60524	0.44587
592.1	-7.77987	14.71690	-9.32613	3.70749	-2.57171	2.71506	0.07056	0.19258
607.5	-8.64489	17.28040	-11.50160	4.16955	-1.55001	1.62244	-0.17551	0.46586
622.9	-9.08175	17.78540	-11.49600	4.02732	-2.09075	3.46496	-2.08015	0.96649
626.8	-9.23512	17.96860	-11.48860	3.99092	-2.95540	5.11948	-3.17919	1.19279
642.2	-8.49238	16.39830	-10.21360	3.63301	-2.79795	4.97881	-3.22982	1.17818
653.8	-8.67412	16.60160	-10.16270	3.58325	-2.60434	4.84362	-3.26884	1.17508
673.1	-8.34392	15.61470	-9.24747	3.34505	-2.38215	4.68220	-3.31299	1.17899
700.1	-8.11999	14.70320	-8.28129	3.07261	-3.04963	6.00161	-4.15036	1.32783
773.4	-8.84206	14.89430	-7.47945	2.72664	-6.52382	11.89320	-7.29197	1.81489
792.7	-8.07406	13.21860	-6.26141	2.45041	-6.80271	12.16550	-7.26979	1.76042
796.6	-8.09848	13.24850	-6.25697	2.44620	-7.07512	12.43710	-7.30007	1.74078
819.7	-6.92696	11.04050	-4.81833	2.14726	-7.51193	12.93670	-7.36310	1.69428
823.6	-6.90009	11.02860	-4.81791	2.15004	-8.93648	15.36260	-8.69818	1.93105
839.0	-5.81089	9.06709	-3.58298	1.90198	-8.41799	14.08970	-7.69270	1.68256
854.4	-5.70658	9.05277	-3.58028	1.90761	-7.78985	12.52810	-6.42462	1.36713
866.0	-5.39525	8.82061	-3.56082	1.92901	-8.93107	14.30270	-7.18236	1.45594
873.7	-5.06939	8.59429	-3.59809	1.96795	-9.21801	14.64460	-7.14817	1.40112
881.4	-2.95035	5.22971	-1.89173	1.69149	-9.52753	15.36190	-7.48314	1.44098
889.2	-2.48271	4.77140	-1.95344	1.77234	-8.82776	14.45550	-6.96085	1.33097
896.9	-2.24223	4.35979	-1.92279	1.81947	-8.17082	13.94060	-6.92474	1.36528
900.7	-2.25113	4.25175	-1.90606	1.83390	-7.79154	13.58860	-6.89739	1.39158
904.6	-2.39820	4 28211	-1.89993	1.83720	-5.89945	10.28500	-5.02695	1.04472
908.4	-2.63008	4.39698	-1.89323	1.83153	-4.58018	7.93223	-3 69776	0.80028
923.9	-3.59770	5.05302	-1.81566	1.75682	-2.66749	3.73836	-1.11329	0.30347
931.6	-5.91220	9.37119	-4.40057	2.26735	-3.28185	4.20608	-1.14976	0.27911
939.3	-5.71805	9.27445	-4.41177	2.28560	-5.69773	8.32445	-3.50538	0.72900
947.0	-5.47458	9.13063	-4.42821	2.31277	-5.99696	8.55615	-3.47890	0.70201
958.6	-5.17888	8.95677	-4.44576	2.34516	-7.78674	11.84630	-5.45358	1.10746
970.2	-4.86259	8.73444	-4.44761	2.37197	-7.94122	11.97960	-5.42050	1.10454
985.6	-4.32036	8.33869	-4.43615	2.39022	-8.21325	12.30610	-5.40639	1.07593
989.5	-4.14291	8.21839	-4.47556	2.42094	-8.24098	12.38630	-5.41611	1.06343
997.2	-1.13104	2.89876	-1.40488	1.85834	-8.15310	12.37050	-5.42453	1.07623
1008.8	-0.60821	2.46909	-1.45655	1.93433	-7.87006	12.21370	-5.41544	1.12463
1028.0	-2.62957	6.57080	-4.30917	2.55102	-4.92806	7.66721	-2.91757	0.72919
1043.5	-3.41984	7.94571	-5.42218	2.79902	-6.28001	10.81400	-5.14684	1.27254
1055.1	-3.39867	7.79731	-5.46827	2.79703	-5.74566	10.19480	-5.14534	1.36474
1070.5	-2.84654	6.35578	-4.43049	2.53272	-8.31126	15.36080	-8.86677	2.23468
1085.9	-1.20077	3.17491	-2.15555	1.95448	-8.10906	14.94940	-8.83898	2.30492
1101.3	-1.47216	3.67970	-2.13973	1.80912	-7.54652	14.55630	-8.93116	2.38251
1109 1	-1.01369	2.51544	-1.12167	1.51184	-7.31772	14.45810	-8.93701	2.37656
1132.2	-1.60928	1.91447	0.30125	0.96824	-7.46093	15.01600	-8.95446	2.24734
1147.6	0.75249	-3.36249	3.82344	0.19234	-9.03492	16.73430	-9.01846	2.03240
1166.9	2.50994	-6.12708	4.88735	0.07429	-6.92469	11.35660	-4.80312	0.97420
1193.9	1.80944	-3.83946	2.57110	0.70030	-6.88804	11.32780	-4.84793	0.92008
1217.1	0.83529	-1.60029	0.67771	1.18969	-4.50708	7.01564	-2.44757	0.44280
1236.4	1.17079	-1.92641	0.57286	1.27836	-5.06380	8.32558	-3.62575	0.71552
1248.0	-0.18571	0.67462	-1.06722	1.62716	-5.33516	9.14736	-4.43345	0.91394
1259.5	-0.28732	0.77114	-1.04632	1.62111	-5.65669	10.07190	-5.28098	1.12154
1271.1	-0.59409	1.03877	-1.00419	1.58947	-5.44116	9.86191	-5.31532	1.14799
1282.7	-0.94794	1.33062	-0.95781	1.55285	-5.38566	9.80572	-5.32997	1.15273
1302.0	-0.03895	-0.84651	0.60731	1.22031	-6.89079	12.32870	-6.74765	1.40862
1321.3	1.06787	-3.03472	1.95884	0.96448	-7.84082	13.54220	-7.27062	1.47727
1348.3	2.30117	-5.02471	3.02235	0.78622	-6.30659	10.17820	-5.12543	1.04174
1363.7	2.48726	-5.13188	3.00710	0.80370	-6.40686	10.24740	-5.17396	1.05242
1398.4	2.80371	-5.31506	3.01011	0.82471	-5.55548	8.66303	-4.29005	0.88476
1456.3	3.11575	-5.47453	2.99547	0.85709	-4.95096	7.73892	-3.87980	0.81724
1521.9	3.17018	-5.41839	2.96934	0.88033	-3.33768	5.05849	-2.45525	0.56102
1541.2	2.90783	-4.94859	2.71762	0.93340	-3.22482	4.96843	-2.46939	0.57425
1579.8	2.60374	-4.48734	2.54039	0.97253	-3.04116	4.81445	-2.48645	0.60610
1595.2	2.70250	-4.76036	2.77554	0.92208	-2.99967	4.77201	-2.48427	0.61985
1618.3	2.06506	-3.67797	2.21037	1.02338	-2.93902	4.70202	-2.47451	0.64836
1637.6	1.28360	-2.39547	1.58265	1.10936	-3.42812	5.64601	-3.05455	0.78376
1672.4	1.21557	-2.67319	2.02612	0.94700	-5.12546	8.41929	-4.41526	1.00493
1707.1	4.47082	-8.50023	5.35771	0.31055	-6.70333	10.71410	-5.38433	1.13008
1726.4	5.74943	-10.54150	6.36525	0.13874	-5.50881	8.35529	-3.89319	0.83132
1757.2	6.81218	-12.08040	7.03336	0.02595	-3.58022	4.76354	-1.74853	0.41122

Table 5. (continued)

cm^{-1}	Parameters for n Using Equation 7				Parameters for k Using Equation 8			
	p_3	p_2	p_1	p_0	q_3	q_2	q_1	q_0
1815.1	6.86090	-11.64880	6.49595	0.14499	-1.41799	1.08996	0.23794	0.03222
1869.1	5.76583	-9.41223	5.06203	0.42830	0.46970	-2.04275	1.91572	-0.29519
1930.8	4.79549	-7.58332	3.96866	0.64563	0.83999	-2.33011	1.86752	-0.27947
1988.7	3.75641	-5.68070	2.85143	0.87224	1.95677	-4.20398	2.90128	-0.48527
2054.3	3.33649	-4.94671	2.45642	0.95304	2.51462	-4.96380	3.21762	-0.53167
2146.9	2.41062	-3.42004	1.66428	1.09397	2.47499	-4.59579	2 88226	-0.45533
2197.1	1 70377	-2.35449	1.14313	1 17886	3.12713	-5.69439	3.52096	-0.58194
2270.4	0 50661	-0.35283	0.02151	1.38851	2.82725	-5.32140	3.39571	-0.57789
2332.1	0.26758	0 24717	-0.41465	1.48641	2 42046	-4.70992	3.09985	-0 53777
2397.7	0.13819	0.54608	-0.60691	1.52758	2.88294	-5.35702	3.41192	-0.59647
2548.1	-0.73071	2.02832	-1.51424	1 73245	3.11780	-5.66359	3 61493	-0.65546
2679 3	-2.60994	5.43468	-3.60233	2.16688	2.92822	-5.23455	3.31225	-0.58233
2845.2	-4.45891	8.76973	-5.71029	2.61759	0.57060	-0.86428	0.71165	-0.06945
2976.4	-4 65069	9.16485	-6 16751	2.77244	-1.23006	2.51907	-1.45062	0.39794
3026.6	-4.52896	8.99669	-6.16317	2.79886	-2.45756	4.87438	-2 99931	0.74210
3092.1	-4.00808	8 00504	-5.61074	2.70731	-3.50045	6.96983	-4.50950	1.11897
3242.6	-1.25046	2.46500	-1.87799	1.84352	-5.01595	10.09690	-6.97952	1.81431
3350.6	1 03561	-2.16592	1.42823	0.99404	-4.58141	9.08774	-6.38503	1.73113
3396.9	1.98777	-4.05762	2.79852	0.62133	-4.08360	8.06910	-5.71285	1.57884
3443.2	2.73412	-5 47136	3.80833	0.33792	-2 97246	5.81053	-4.16988	1.20699
3485.7	3.21854	-6 37206	4.45282	0.15543	-2 00143	3.84710	-2.79142	0 85045
3489.5	3.18554	-6.34032	4.45572	0.14853	-1.37803	2 68801	-2.07430	0.70053
3493.4	3.19557	-6.34126	4.45379	0.14653	-1.95365	3 72945	-2 68390	0.81261
3497.2	3.21301	-6.35408	4.45180	0 14750	-1.29787	2.51972	-1 94246	0.65911
3539 7	3.22176	-6.32681	4.44780	0.13352	-0.50104	0.88749	-0 75127	0.32874
3547.4	2.62881	-5.19686	3.74403	0.27687	-0.56308	0.95968	-0.74925	0.30911
3586.0	2.44754	-4.74509	3.39150	0.37079	0.49370	-1 02757	0.56499	-0.02103
3593.7	1.99316	-3.88595	2 85703	0.48256	0.20979	-0.51582	0.27734	0.02308
3609.1	2.05137	-3.94734	2 85418	0.49953	0.20647	-0.48339	0.27051	0.00573
3620.7	1 69213	-3.24572	2.39651	0.60423	0.19909	-0.45777	0.26657	-0.00633
3632.3	1.70539	-3.26955	2.39947	0 61421	0.20736	-0.44716	0 26178	-0.01526
3647.7	1.73032	-3 30906	2.40255	0 62947	0 19463	-0.41731	0.25869	-0 02770
3701.7	1.34616	-2.59447	1.90504	0.78007				
3802 0	0 37163	-0.73395	0 68201	1.08246				
3902 3	0 02954	-0.05203	0 21098	1.20979				
3998 8	0 07116	-0.11714	0 22802	1 22542				
4500.4	0 14876	-0.20531	0.22182	1 27636				
5001.9	-0 14076	0 31885	-0.09364	1 35646				
5499.6	-0.39719	0 79761	-0 38850	1.42686				
6001.2	-0.24803	0.51121	-0.20830	1.39703				
6498.9	-0.10040	0.23812	-0.04143	1 36858				
6996.6	-0.36325	0.71679	-0.32737	1 42854				
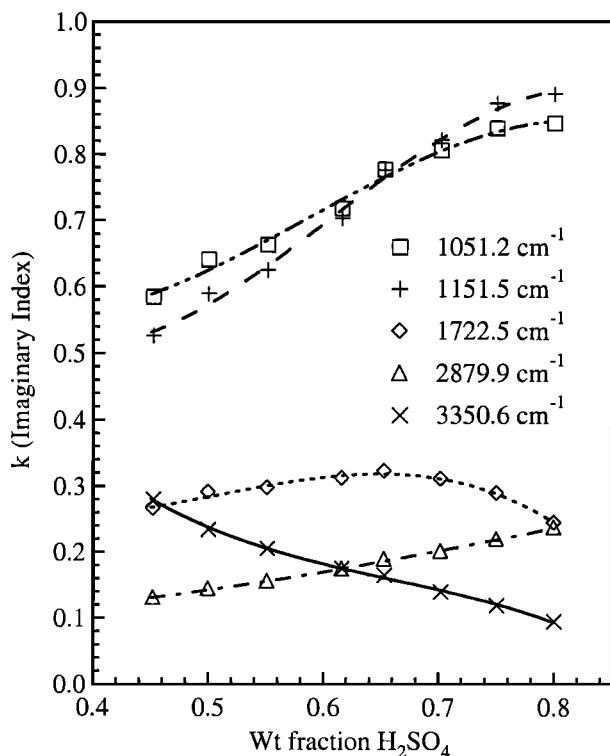
crease in the imaginary index, two cases of a constant imaginary index were assumed, one with k=3x10^{-3}, the other with k=1x10^{-3}. In both cases, the real indices obtained differed by less than 1% from those obtained using the exponentially decreasing imaginary index.

The final model test examined the assumption that we have a film on the back side of the wafer which is 1% of the thickness of the film on the front side. Optical constants were determined for 75 wt% H_2SO_4 using 0.1 and 10% film thickness ratios on the back side of the wafer for comparison with the reported data. The calculated spectra from the 0.1% film thickness ratio determination match the calculated spectra nearly identically, and the determined imaginary indices were all within 1.3 % of those determined using the 1% film thickness ratio. We therefore conclude that if our film thickness ratio is an overestimate, the errors are much lower than some of the previous sources of error. The 10% film thickness ratio gives larger dif-

Figure 8. A plot of the variation of the imaginary refractive index with wt% for a few frequencies corresponding to peaks in the H_2SO_4 spectrum. The points are the data, and the curves are fits to the data using equation 8.
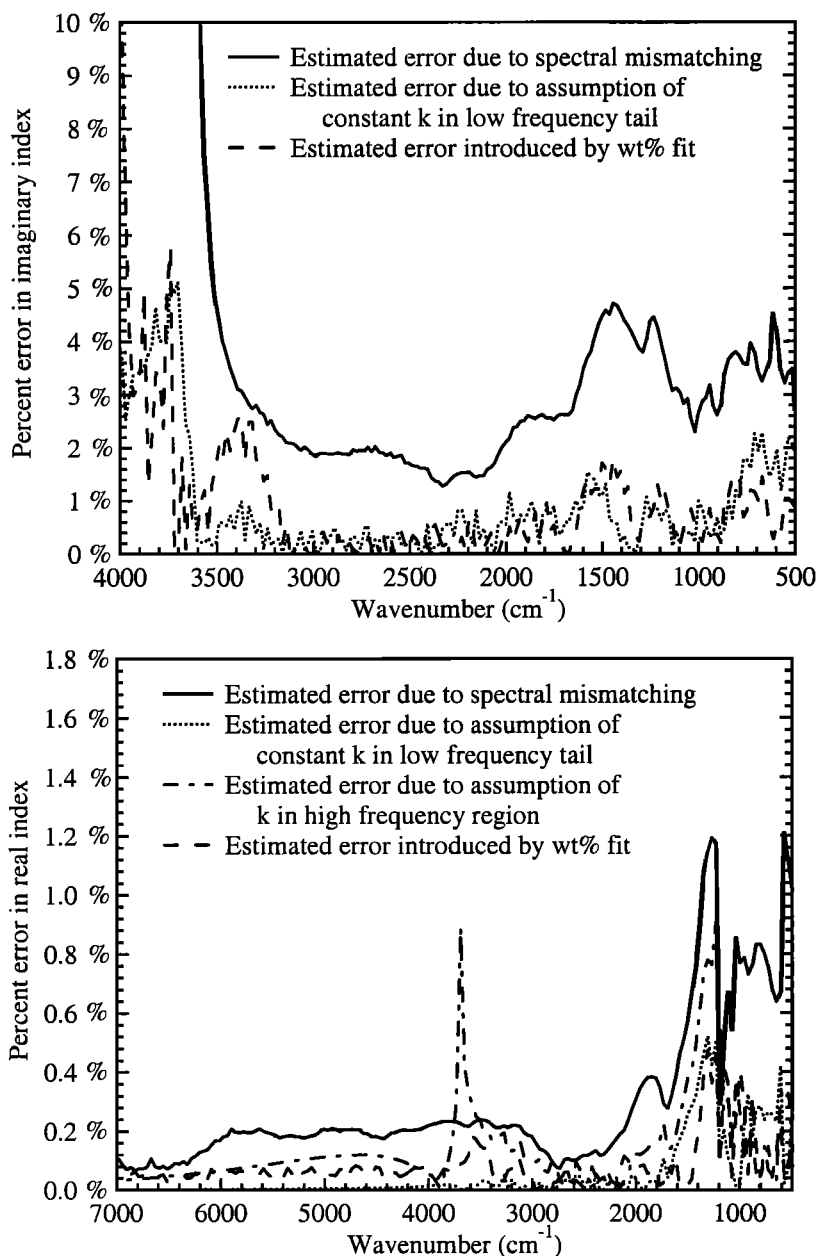
Figure 9. A plot of the percent difference between the real and imaginary refractive indices for 75 wt% H_2SO_4 determined by several methods, as shown in the legend and described in the text.

ferences between the measured and calculated spectra, and the determined imaginary indices are as much as 10% lower than those determined using the 1% film thickness ratio, although the mean difference was only 2% lower. However, the calculated spectra fit the measured spectra very poorly in the 4000-7000 cm^{-1} region , indicating that the film thickness ratio is certainly not 10% and is most likely less than 5%. Hence we conclude that if the film thickness ratio were greater than 1%, it would result in less than a 2% change in the imaginary refractive index for most frequencies.

The interpolation between frequencies and compositions will theoretically add error to the measured values. To quantify the error from frequency interpolation, the indices calculated by interpolation were compared with the measured indices. The errors introduced are small, and the mean and maxi-

mum errors are reported in Table 4 for each composition studied. The error due to interpolation in composition can be estimated by calculating the indices for each composition studied using the fit parameters reported in Table 5. The mean and maximum errors from the composition interpolation are listed in Table 4 for each composition studied, and the percent error in the indices for 75 wt% H_2SO_4 is shown as a function of frequency in Figure 9. These errors are higher than those for frequency interpolation.

We conclude that the spectral matching error is larger than all other sources of error. We therefore estimate that, in general, our measured real and imaginary indices are accurate to within 0.5 and 5%, respectively, for frequencies less than 3500 cm^{-1}. One exception to this is for the imaginary indices of 45 wt% H_2SO_4, which we believe are accurate to within 10%.

Table 6. Estimated Errors From Spectral Mismatching and Error-Weighting Methods

	Percent Error From Spectral Mismatch				Percent Error from Error Weighting Method			
	Mean		Maximum		Mean		Maximum	
Nominal wt%	n	k	n	k	n	k	n	k
45.2	0.4	6.5	1.9	14.4	0.2	2.8	1.0	7.2
50.0	0.2	2.9	1.3	13.9	0.1	1.3	1.1	10.5
55.1	0.3	2.3	1.7	6.5	0.2	2.0	2.0	6.5
61.6	0.3	3.3	1.7	7.3	0.2	1.8	1.3	8.4
65.3	0.2	1.9	1.1	6.1	0.1	0.8	0.8	5.4
70.2	0.2	2.2	0.9	21.8	0.1	0.7	0 7	4.7
75.0	0.3	3.1	1.3	21.5	0.1	0.6	0.6	3.1
80.0	0.3	2.2	1.5	12.2	0.1	1.3	0 9	10.7

The other exception is for the imaginary indices of all compositions at frequencies above 3500 cm⁻¹, which we believe are accurate to within only 20%. If frequency interpolations are used on the data, additional minimal errors can be introduced, especially if frequency interpolations are made on the fit parameters used to calculate the indices at compositions other than those measured. For this reason, we recommend that if the composition fits are to be used at frequencies other than those for which they are reported in Table 5, the fit parameters for those frequencies be obtained from the full data set, which is available as supplementary material through this journal.

7. Conclusions

We have determined the optical constants of sulfuric acid solutions at 5 wt% intervals between 45 and 80 wt% H₂SO₄ at 215 K. The frequency ranges reported are 7000-500 cm⁻¹ and 3650-500 cm⁻¹ for the real and imaginary refractive indices, respectively. These low-temperature optical constants are significantly different from those measured at room temperature, especially for compositions below 75 wt% H₂SO₄, and should assist studies which rely on accurate measurements of the optical constants. An interpolation scheme has been created to allow calculation of optical constants at compositions between the compositions of our measurements.

There are several sources of error in our measurements, resulting in difficulties in estimating the overall error. We estimate that, in general, our measured real and imaginary refractive indices are accurate to within 0.5 and 5%, respectively, with a few exceptions discussed in the previous section. We recommend that the fit parameters determined in this study be used to calculate the optical constants rather than using the measured data.

References

Anthony, S. E., R. T. Tisdale, R. S. Disselkamp, and M. A. Tolbert, FTIR studies of low-temperature sulfuric acid aerosols, *Geophys. Res Lett.*, *22*, 1105-1108, 1995.

Beyer, K. D., A. R. Ravishankara, and E. R. Lovejoy, Measurements of UV refractive indices and densities of H₂SO₄/H₂O and H₂SO₄/HNO₃/H₂O solutions, *J. Geophys. Res.*, *101*, 14,519-14,524, 1996.

Clapp, M. L., R. F. Niedziela, L. J. Richwine, T. Dransfield, R. E. Miller, and D. R Worsnop, Infrared spectroscopy of sulfuric acid/water aerosols: Freezing characteristics, *J. Geophys. Res.*, *102*, 8899-8907, 1997.

Grainger, R. G., A. Lambert, C. D. Rogers, F. W. Taylor, and T. Deshler, Stratospheric aerosol effective radius, surface area, and volume estimated from infrared measurements, *J. Geophys. Res.*, *100*, 16,507-16,518, 1995.

Guldan, E. D., L. R. Schindler, and J. T. Roberts, Growth and characterization of sulfuric acid under ultrahigh vacuum, *J. Phys. Chem.*, *99*, 16,059-16,066, 1995.

Hanson, D. R., and A. R. Ravishankara, The reaction probabilities of ClONO₂ and N₂O₅ on 40 to 75% sulfuric acid solutions, *J. Geophys. Res.*, *96*, 17,307-17,314, 1991.

Heavens, O. S., *Optical Properties of Thin Solid Films*, Academic, San Diego, Calif., 1955

Iraci, L. T., A. M. Middlebrook, and M. A Tolbert, Laboratory studies of the formation of polar stratospheric clouds: Nitric acid condensation on thin sulfuric acid films, *J. Geophys. Res.*, *100*, 20,969-20,977, 1995

Kinne, S., O B. Toon, and M. J. Prather, Buffering of stratospheric circulation by changing amounts of tropical ozone: A Pinatubo case study, *Geophys. Res. Lett.*, *19*, 1927-1930, 1992.

Kozima, K., W. Suetaka, and P. N. Schatz, Optical constants of thin films by a Kramers-Kronig method, *J. Opt. Soc. Am.*, *56*, 181-184, 1966

Masterson, C. M, and R. K. Khanna, Absorption intensities and complex refractive indices of crystalline HCN, HC₃N, and C₄N₂ in the infrared region, *Icarus*, *83*, 83-92, 1990.

Middlebrook, A. M., L. T. Iraci, L. S. McNeill, B. G. Koehler, M. A. Wilson, O. W. Saastad, M. A. Tolbert, and D. R. Hanson, Fourier transform infrared studies of thin H₂SO₄/H₂O films: Formation, water uptake, and solid-liquid phase changes, *J. Geophys. Res.*, *98*, 20,473-20,481, 1993.

Minnis, P., E. F. Harrison, L. L. Stowe, G. G. Gibson, F. M. Denn, D. R. Doelling, and W L Smith Jr., Radiative climate forcing by the Mount Pinatubo eruption, *Science*, *259*, 1411-1415, 1993.

Nilsson, P. O., Determination of optical constants from intensity measurements at normal incidence, *Appl Opt.*, *7*, 435-442, 1968.

Palmer, K. F., and D Williams, Optical constants of sulfuric acid; application to the clouds of Venus?, *Appl. Opt.*, *14*, 208-219, 1975

Pearl, J., M. Ngoh, M. Ospina, and R. Khanna, Optical constants of solid methane and ethane from 10,000 to 450 cm⁻¹, *J. Geophys. Res.*, *96*, 17,477-17,482, 1991.

Perry, R. H., and D. W. Green, *Perry's Chemical Engineer's Handbook*, *6th ed.*, pp. 3.85-3.86, McGraw-Hill, New York, 1984.

Pinkley, L. W., and D Williams, The infrared optical constants of sulfuric acid at 250 K, *J. Opt. Soc. Am.*, *66*, 122-124, 1976.

Press, W. P., B. P Flannery, S. A. Teukolsky, and W. T. Vetterling, *Numerical Recipes: The Art of Scientific Computing (FORTRAN Version)*, pp. 298-301, Cambridge Univ Press, New York, 1989.

Querry, M R., R. C. Waring, W. E. Holland, L M. Earls, M. D.

Herrman, W. P. Nijm, and G. M. Hale, Optical constants in the infra-red for K_2SO_4, $NH_4H_2PO_4$, and H_2SO_4 in water, *J. Opt. Soc. Am.*, *64*, 39-46, 1974.

Remsberg, E. R., D. Lavery, and B. Crawford Jr., Optical constants for sulfuric and nitric acids, *J. Chem. Eng. Data*, *19*, 263-265, 1974.

Rinsland, C. P., G. K. Yue, M. R. Gunson, R. Zander, and M. C. Abrams, Mid-infrared extinction by sulfate aerosols from the Mt. Pinatubo eruption, *J. Quant. Spectrosc. Radiat. Transfer*, *52*, 241-252, 1994.

Steele, H. M., and P. Hamill, Effects of temperature and humidity on the growth and optical properties of sulphuric acid-water droplets in the stratosphere, *J. Aerosol Sci.*, *12*, 517-528, 1981.

Tabazedeh, A., O. B. Toon, S. L. Clegg, and P. Hamill, A new parame-terization of H_2SO_4/H_2O aerosol composition: Atmospheric implica-tions, *Geophys. Res. Lett.*, *24*, 1931-1934, 1997.

Tisdale, R. T., A. M. Middlebrook, A. J. Prenni, and M. A. Tolbert, Crystallization kinetics of HNO_3/H_2O films representative of polar stratospheric clouds, *J. Phys. Chem. A*, *101*, 2112-2119, 1997.

Toon, O.B., M. A. Tolbert, B. G. Koehler, A. M. Middlebrook, and J. Jordan, Infrared optical constants of H_2O ice, amorphous nitric acid solutions, and nitric acid hydrates, *J. Geophys. Res.*, *99*, 25,631-25,654, 1994.

Verleur, H. W., Determination of optical constants from reflectance or transmittance measurements on bulk crystals or thin films, *J. Opt. Soc. Am.*, *58*, 1356-1364, 1968.

Warren, S. G., Optical constants of ice from the ultraviolet to the micro-wave, *Appl. Opt.*, *23*, 1206-1225, 1984.

Young, R. E., H. Houben, and O. B. Toon, Radiatively forced dispersion of the Mount Pinatubo volcanic cloud and induced temperature per-turbations in the stratosphere during the first few months following the eruption, *Geophys. Res. Lett.*, *21*, 369-372, 1994.

Yue, G. K., and A. Deepak, Modeling of growth and evaporation effects on the extinction of 1.0-μm solar radiation traversing stratospheric sulfuric acid aerosols, *Appl. Opt.*, *20* 3669-3675, 1981.

D.L. Glandorf, R.T. Tisdale, and M.A. Tolbert, Cooperative Institute for Research in Environmental Sciences, Campus Box 216, University of Colorado, Boulder CO 80309. (e-mail: glandorf@ucsu.colorado.edu; rtisdale@terra.colorado.edu; tolbert@spot.colorado.edu)

O.B. Toon, Laboratory for Atmospheric and Space Physics, Campus Box 392, University of Colorado, Boulder CO 80309. (e-mail: toon@maia.colorado.edu)